JCEC
THE JOURNAL OF ENGINEERING AND EXACT SCIENCES

OPEN ACCESS

The Journal of Engineering and Exact Sciences – jCEC, Vol. 09 N. 04 (2023)
journal homepage: https://periodicos.ufv.br/jcec
eISSN: 2527-1075
ISSN: 2446-9416

Electrical behavior of n-GaAs Schottky nanowire in wide temperature range for different contacts

Article Info:
Article history: Received 2023-01-06 / Accepted 2023-05-20 / Available online 2023-05-24
doi: 10.18540/jcecvl9iss4pp15855-01e

Souad Benykrelef
ORCID: https://orcid.org/0000-0002-9146-0672
Laboratoire de Micro-électronique Appliquée, Université Djillali Liabés de Sidi Bel Abbés, BP 89, Sidi Bel Abbés, 22000, Algeria
E-mail: s.benyekhlef@outlook.fr
Sedik Mansouri
ORCID: https://orcid.org/0000-0002-7946-4507
Laboratoire de Micro-électronique Appliquée, Université Djillali Liabés de Sidi Bel Abbés, BP 89, Sidi Bel Abbés, 22000, Algeria
E-mail: s_mansouridz@yahoo.fr
Hicham Helal
ORCID: https://orcid.org/ 0000-0002-3682-1957
Laboratoire de Micro-électronique Appliquée, Université Djillali Liabés de Sidi Bel Abbés, BP 89, Sidi Bel Abbés, 22000, Algeria
E-mail: hichamwartilani@yahoo.com
Abdelaziz Rabehi
ORCID: https://orcid.org/ 0000-0001-8684-4754
Laboratoire de Micro-électronique Appliquée, Université Djillali Liabés de Sidi Bel Abbés, BP 89, Sidi Bel Abbés, 22000, Algeria
Wireless and Wired Communication and Smart Systems Laboratory, Djelfa university of Algeria, Djelfa, 17000, Algeria
E-mail: rab_ehi@hotmail,fr
Abdelaziz Joti
ORCID: https://orcid.org/ 0000-0001-8635-9919
Laboratoire de Micro-électronique Appliquée, Université Djillali Liabés de Sidi Bel Abbés, BP 89, Sidi Bel Abbés, 22000, Algeria
E-mail: jotiabdelaziz@hotmail.com
Zineb Benamara
ORCID: https://orcid.org/ 0000-0003-0017-2550
Laboratoire de Micro-électronique Appliquée, Université Djillali Liabés de Sidi Bel Abbés, BP 89, Sidi Bel Abbés, 22000, Algeria
E-mail: benamara20022000@yahoo.fr

Abstract
This research aims to study the impact of metal work function ϕ_m on the I–V characteristics of a n-GaAs Schottky nanowire structure, using 3D Silvaco-Atlas software. The electrical characteristics have been performed in a wide temperature range of 300-550K. This allows us to study and discuss the influence of temperature and the metal work function ϕ_m on the performance of our proposed device. The results show a great dependence between ϕm and the electrical parameters. A decrease in current is observed with increasing ϕ_m, as well as an increase in barrier height with increasing ϕm and a decrease with increasing temperature.
Keywords: n-GaAs; nanowire; Silvaco-Atlas; Schottky diode; the I–V characteristics.

1. Introduction

Silicon is the primary material used in the manufacture of semiconductors today, and CMOS technology will likely continue to dominate the electronics market for many decades to come (Lin *et al.*, 2014). But as the size of transistors shrinks, metal contacts and interconnects have become one of the most important problems.

III-V semiconductor nanowires constitute a new class of nanoscale materials. They are considered the next frontier for ultrasmall, highly efficient semiconductors and therefore are widely studied in the context of electronic devices, optoelectronics (Saxena *et al.*, 2013; Yang al., 2010), and nano-photonic circuits (Yan *et al.*, 2009; Pauzauskie *et al.*, 2006), such as LEDs, nano-lasers, optical switches (Law *et al.*, 2004; Mayer *et al.*, 2013), and waveguides. An active cylindrical III-V nanowire with a diameter of a few hundred nanometers and a length of micrometers can effectively limit and guide optical waves inside the nanometer-scale gain medium, and it can also enable the optical integration of III-V semiconductor assets on existing silicon technologies.

Future progress of these devices will depend on fabricating nanowires with precise control of their morphology, crystal structure, composition, doping, and quantum efficiency.

Our work proposes an original strategy to study the Schottky contact metal effect on the electrical behavior of the n-GaAs Schottky nanowire in low and high temperatures, using Silvaco-Atlas software.

The current-voltage (I-V) characteristics of microelectronic devices provide fundamental parameters such as factor n, barrier height Φ_b, and series resistance R_S. There are several methods to determine these parameters, such as Cheung and Cheung, Norde, and classical methods, but unfortunately there are some disagreements with him. As a result, we chose the Helal method (Helal *et al.*, 2020 a), which is valid in low and high voltage as well as a wide temperature range.

The structure is studied for different metal work functions ranging from 4.33 to 5.93 eV, for different temperatures (300°-550°K). The electrical parameters Φ_b, n and R_S are extracted for each temperature, and we study their evolution according to the temperature.

2. Simulation part

The geometry of the n-GaAs Schottky nanowire structure is chosen according to the realistic fabrication process described by Wang *et al.* (20130 and Wu *et al.* (2016). The n-GaAs is of 200 nm diameter and 1.5 µm length, with a concentration doping of $Nd = 5\times10^{17}$ cm^{-3}. The Schottky and ohmic contacts are defined on the top and back sides, respectively, with 0.3 µm of thickness. The 3D technological characteristics of the n-GaAs Schottky nanowire simulated are illustrated in Figure.1:

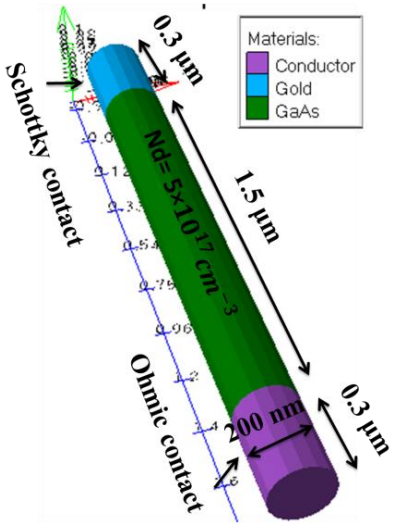

Figure 1. 3D structure of n-GaAs Schottky nanowire

The effect of the interface states is neglected by taking low densities for donor and acceptor states of 1×10^{10} cm^{-2} eV^{-1}. The work function of the Schottky contact is varied from 4.5 to 5.3 eV. The Silvaco-Atlas software takes into account all of the electrical properties of n-GaAs and its contacts, such as forbidden band properties *Eg*, electron affinity χ, dielectric constant ε, density of conductance states *Nc*, density of valance states *Nv*, electron mobility μn, hole mobility μp, work function of the metals Φ_m, etc., and uses the Poisson equation and the Continuity equation for electrons and holes as basic equations for the transport mechanisms.

The Poisson equation is expressed as:

$$div(\varepsilon \nabla \Psi) = \rho \quad (1)$$

Where, Ψ is the electrostatic potential, ε is the permittivity and ρis the space charge density.

The continuity equations are given by:

$$\frac{\partial n}{\partial t} = \frac{1}{q} div\, j_n + g_n - r_n \quad (2)$$

$$\frac{\partial p}{\partial t} = \frac{1}{q} div\, j_p + g_p - r_p \quad (3)$$

q is the electron charge, n and p are the electrons and holes concentrations, j_n and j_p are the electron and hole current densities, r_n and r_p are the recombination rates for electrons and holes, g_n and g_p are the generation rates for electrons and holes.

The models used in this simulation are the Shockley-Read-Hall "SRH" recombination (Selberherr *et al.*, 2012). Auger recombination rate "Auger" (Caughey *et al.*, 1967) and concentration dependent mobility "CONMOB" (Selberherr *et al.*, 1984). The numerical resolution methods are the Gummel and Newton methods. Finally, the temperature is varied from 300° to 550° K with a step of ΔT = 50 K.

3. Results and discussions

Figures (2-6) show that the structure presents the behavior of Schottky contact for all values of the Φm. It is observed that the current increases linearly with bias voltage and it decreases progressively with an increase of Φ_m.

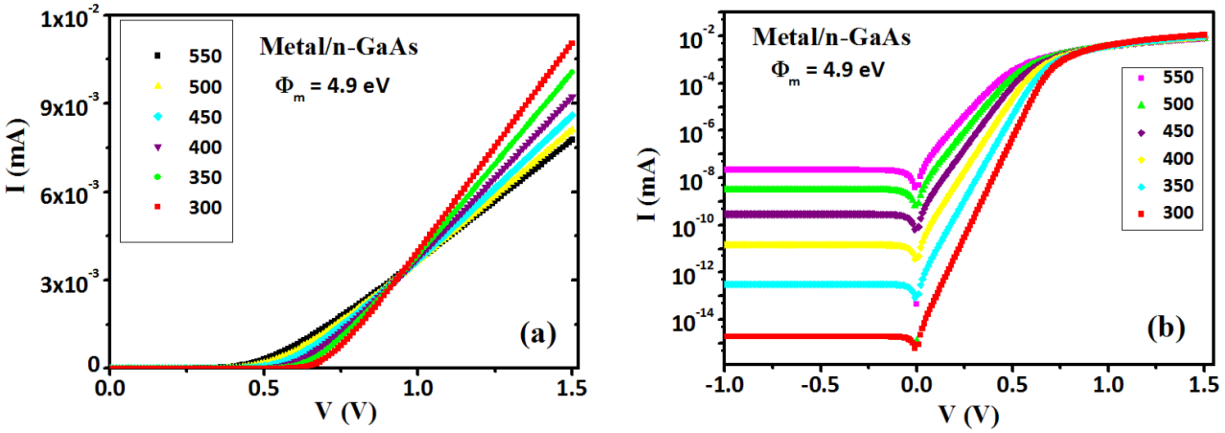

Figure 2. (a) Linear forward bias I-V, (b) Semi-logarithmic I-V characteristics of n-GaAs Schottky nanowire for different temperatures (Φ_m =4.9 eV)

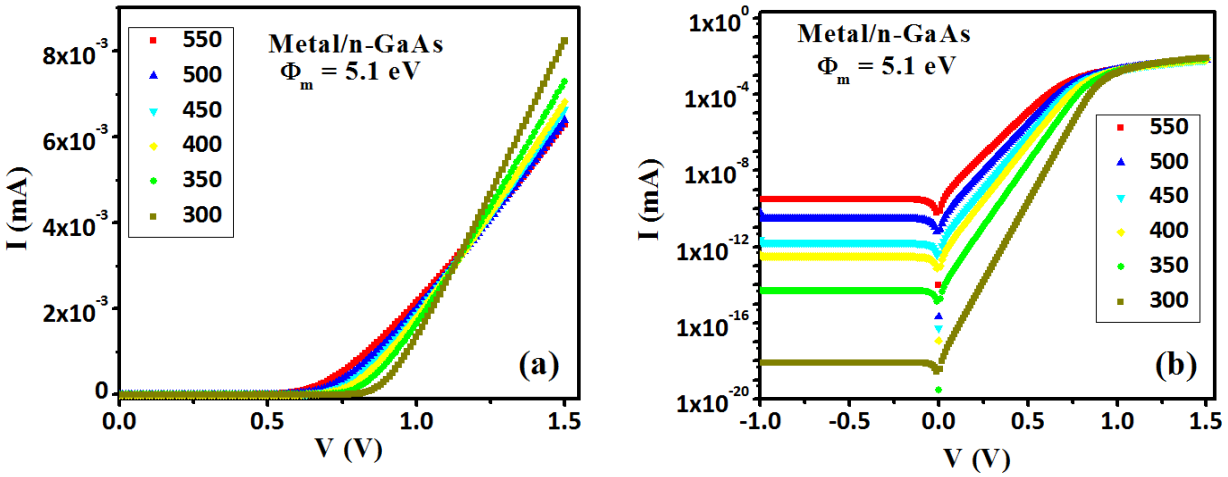

Figure 3. (a) Linear forward bias I-V, (b) Semi-logarithmic I-V characteristics of n-GaAs Schottky nanowire for different temperatures (Φ_m=5.1 eV)

For the reverse bias voltage, the reverse current I_r decreases with the increase of Φ_m and increasing temperature. For the forward and low bias voltage, the current increases linearly with bias voltage and shifts gradually toward the higher bias side with an increase of Φ_m. At high bias voltage, the linearity is deviated with an increase in bias voltage due to the effect of the series resistance (Helal *et al.*, 2020 b; Helal *et al.*, 2019).

The current across the Schottky contacts is the thermionic emission mechanism, which is expressed by (Rhoderick *et al.*, 1988; Sze *et al.*, 2006):

$$I = I_s\left(exp\left(\frac{q(V-IR_S)}{nkT}\right)-1\right) \quad (4)$$

where I_s is the saturation current expressed as:

$$I_S = AA^*T^2exp\left(-\frac{q\Phi_b}{kT}\right) \quad (5)$$

where R_s is the series resistance, n is the ideality factor, k is the Boltzmann constant, T is the temperature, A is the effective diode area equal 2.8×10^{-5} cm^{-2}, Φ_b is the barrier height and A^* is the effective Richardson constant.

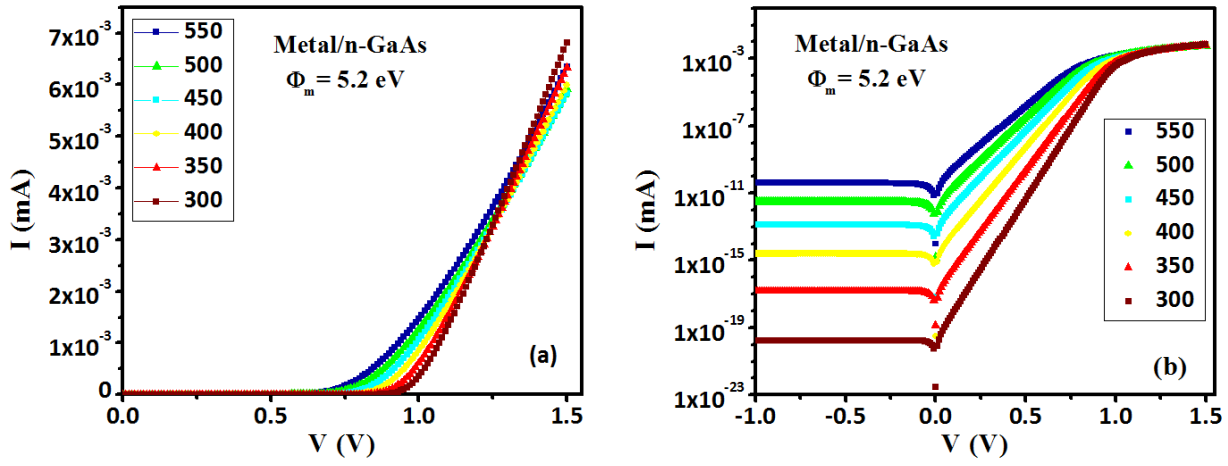

Figure 4. (a) Linear forward bias I-V, (b) Semi-logarithmic I-V characteristics of n-GaAs Schottky nanowire for different temperatures (Φ_m=5.2 eV)

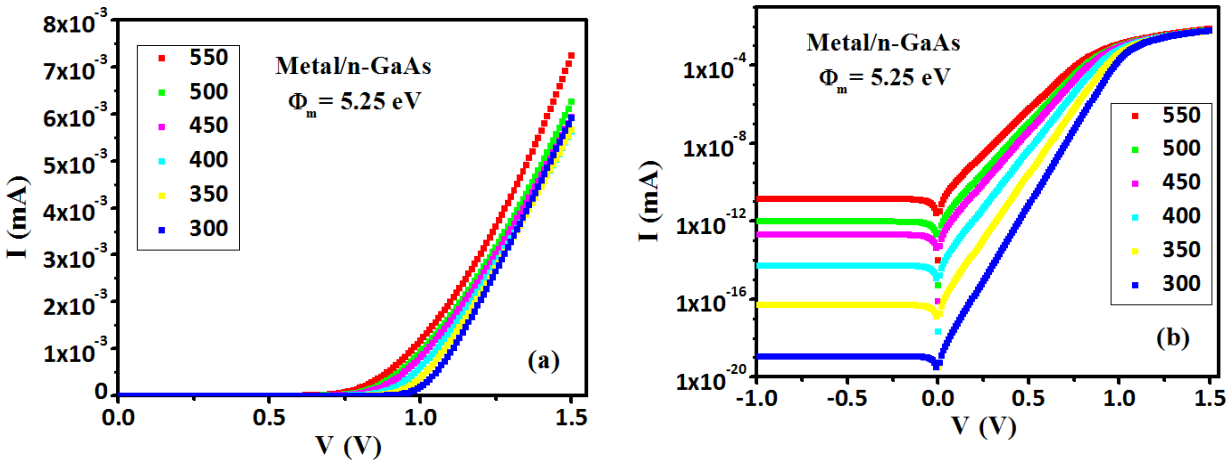

Figure 5. (a) Linear forward bias I-V, (b) Semi-logarithmic I-V characteristics of n-GaAs Schottky nanowire for different temperatures (Φ_m=5.25 eV)

The electrical parameters such as ideality factor n, barrier height Φ_b, series resistance R_s and saturation current I_s are extracted from the forward I-V characteristics using Helal method by the following expressions (Helal *et al.*, 2020 a):

$$I = AA^*T^2\, exp\left(\frac{-q\phi_b}{kT}\right) exp\left(\frac{q(V-R_sI)}{kT}\right)\ exp\ \left(-\frac{1}{n}\right) \tag{6}$$

$$V = \frac{kT}{q} ln(I) - \frac{kT}{q} ln(A.A^*T^2) + \phi_b + \frac{kT}{qn} + R_s exp\ (ln\ I) \tag{7}$$

$$h_1(ln(I)) = \frac{\partial V}{\partial (lnI)} = \frac{kT}{q} + R_s exp\ (ln\ (I)) \tag{8}$$

R_s and n are calculated from the slope and intercept with the y-axis of the h_1 versus I plot, respectively.

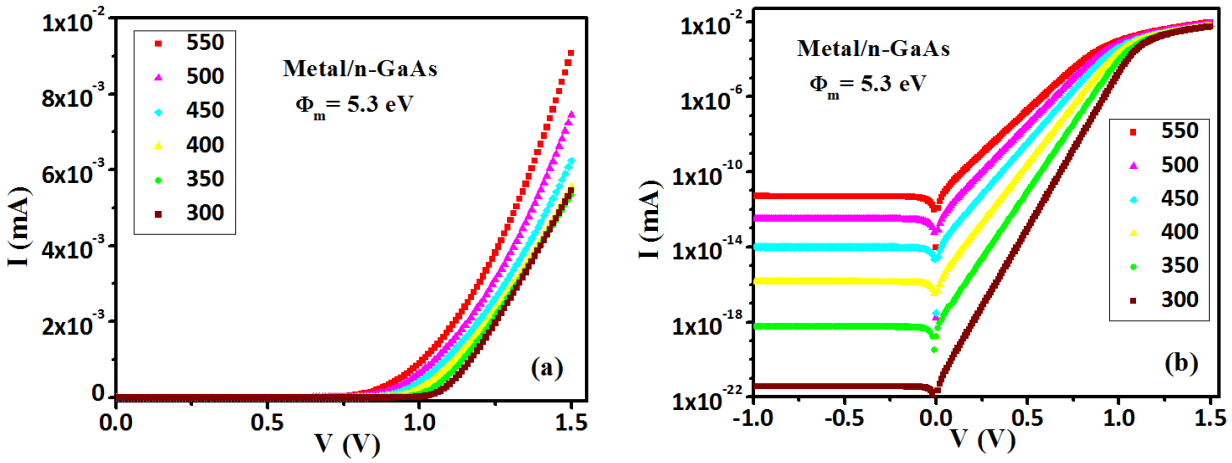

Figure 6. (a) Linear forward bias I-V, (b) Semi-logarithmic I-V characteristics of n-GaAs Schottky nanowire for different temperatures (Φ_m=5.3 eV)

We extract the values of barrier height from the relation $h_2(I)$, which is expressed as:

$$h_2(I) = V - \frac{kT}{q} ln\left(\frac{I}{AA^*T^2}\right) - \frac{kT}{qn} = R_s I + \phi_b \quad (9)$$

R_s and φ_b are calculated from the slope and intercept with the y-axis of the h_2 versus I plot, respectively.

The variation of the ideality factor n versus T in high and low voltage for different work function (Φ_m), are presented in Figures 7.

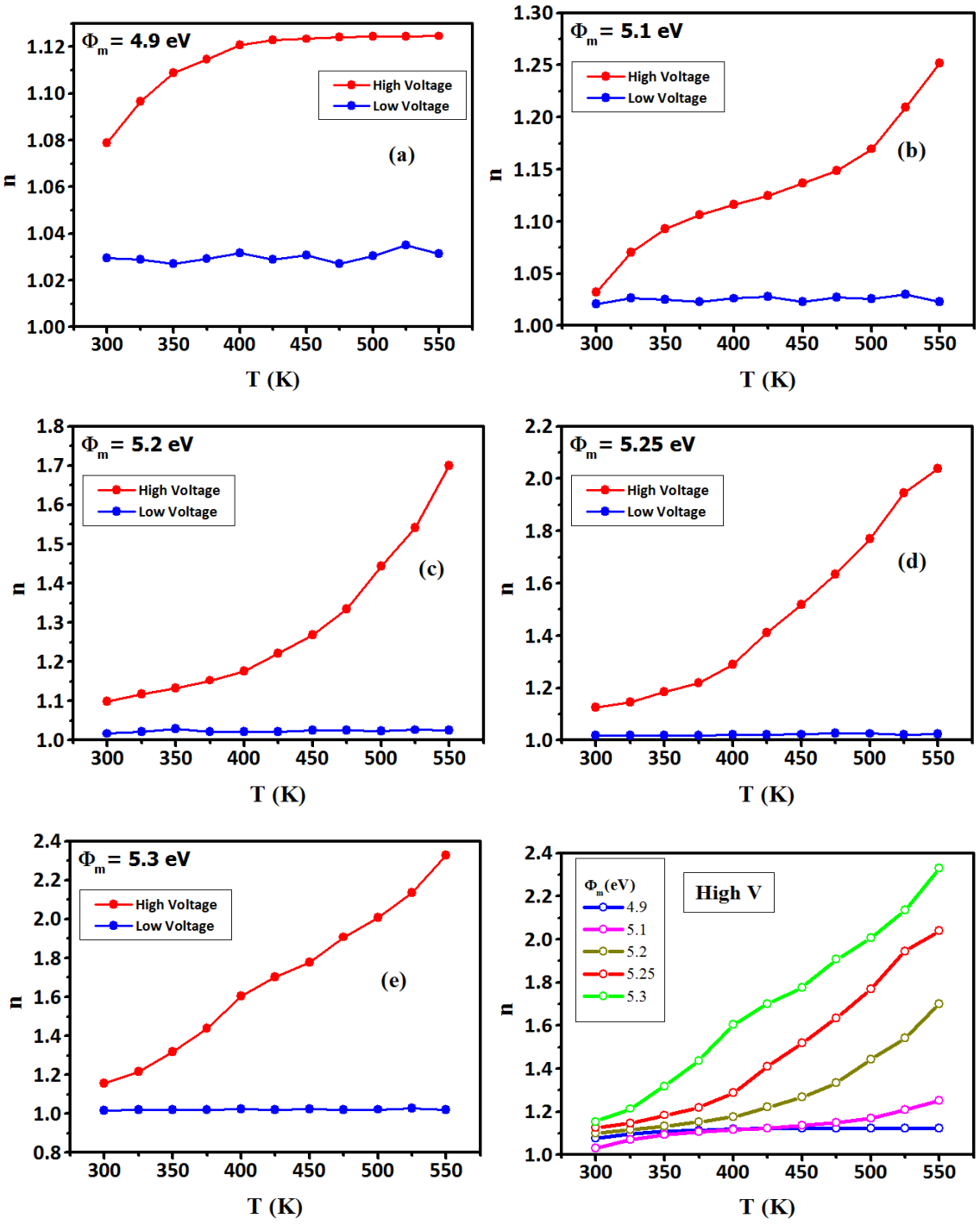

Figure 7. Ideality factor (n) versus T(°K) for different works function in high voltage

Figure 7, shows the variation of the ideality factor n at a different temperature, for low voltage, the ideality factor n is around 1 for all values of work function ϕ_m, but for high voltage the n values increase with increasing temperature and ϕ_m. In most of studies *n* decreases with the increase of temperature, because *n* was extracted from the low voltage part lower than 0.9 V, for us we have other mechanisms like tunnel effect which dominates the high voltage and becomes more dominant with increasing temperature.

The series resistance R_s is an important parameter in the study of Schottky barrier diodes because it limits the conduction process (Ahaitouf *et al.*, 2012). This parameter has been determined versus Φ_m and shown in Figure 8.

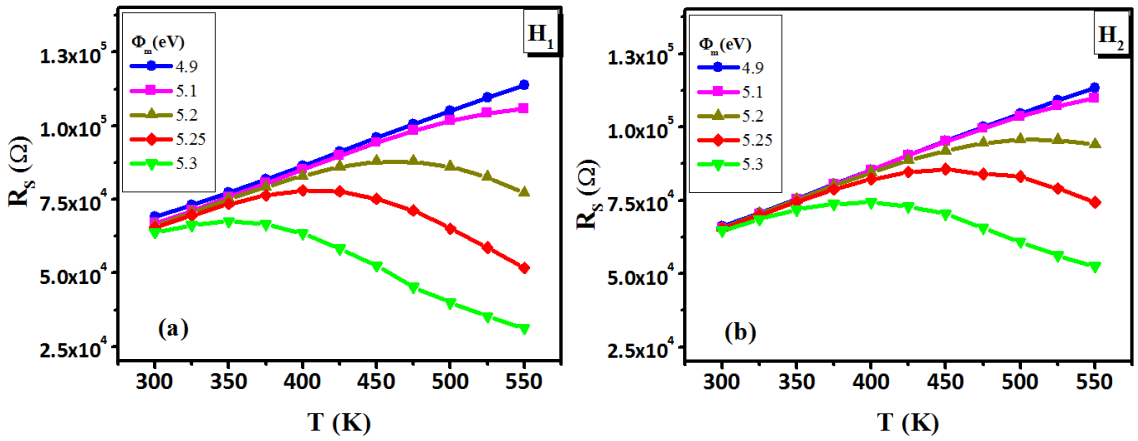

Figure 8. Series resistances T(K) for different works function (a) Using H_1(I) method (b) Using H_2(I) method

As can be seen, the values of the series resistance extracted using h_1(I) and h_2(I) methods are very close, which is in concordance with the work of Helal *et al.* (2020 a). We observe that for the contact with low work function (4.9 et 5.1 eV), series resistance is increasing for all temperature range but for Φ_m= (5.2 - 5.25- 5.3) eV R_S is decreasing gradually from (500°K – 450°K – 400°K) respectively. As can be see the large series resistance values of one of our NW varies between (10^4 et 10^5) Ω close to the values found by Núñez *et al.* (2020), but when the NWs will be assembled the total equivalent resistance will decrease considerably.

Fig.9 shows the variation of the barrier height Φ_b versus Φ_m, we can see that the barrier height increases with increasing Φ_m and decreases with increasing temperature what is logical because the Fermi-level pinning at the metal/semiconductor interface. It is well known that the theoretical relationship of Φ_b and Φ_m is given by Helal *et al.* (2020):

$$\Phi_b = \Phi_m - \chi_{sc} \qquad (10)$$

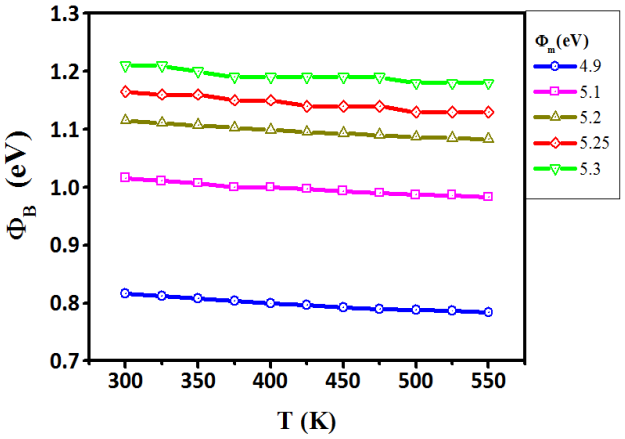

Figure 9. Φ_b versus T(K) of n-GaAs Schottky nanowire for different works function

4. Conclusion

To investigate the effect of metal work function ϕ_m on n-GaAs Schottky nanowire structure, we have using 3D Silvaco-Atlas software in wide temperature range, by Silvaco-Atlas software. we used Helal method to annalyse I(V) characteristics which proves its efficiency for low and high voltage.

The results in high voltage show an increase of the ideality factor with increasing temperature and increasing work function. The lower values of the ideality factor *n*, were found for 4.9 and 5.1 eV.

We observed that the barrier height increases with increasing Φ_m and decreases with increasing temperature. It's also known that for ideal Schottky contacts the dominant current is the thermionic emission (TE) (Helal *et al.*, 2020). But in practical, there are other mechanisms that influence transport phenomena like the effect of tunnel currents and field emission.

References

Ahaitouf, A., Srour, H., Hamady, S. O. S., Fressengeas, N., Ougazzaden, A., & Salvestrini, J. P. (2012). Interface state effects in GaN Schottky diodes. Thin Solid Films, 522, 345-351. doi: https://doi.org/10.1016/j.tsf.2012.08.029

Caughey, D. M., & Thomas, R. E. (1967). Carrier mobilities in silicon empirically related to doping and field. Proceedings of the IEEE, 55(12), 2192-2193. doi: 10.1109/PROC.1967.6123. doi:https://doi.org/10.1038/nphoton.2009.184

Helal, H., Benamara, Z., Arbia, M. B., Khettou, A., Rabehi, A., Kacha, A. H., & Amrani, M. (2020). A study of current-voltage and capacitance-voltage characteristics of Au/n-GaAs and Au/GaN/n-GaAs Schottky diodes in wide temperature range. International Journal of Numerical Modelling: Electronic Networks, Devices and Fields, 33(4), e2714. doi: https://doi.org/10.1002/jnm.2714

Helal, H., Benamara, Z., Arbia, M. B., Rabehi, A., Chaouche, A. C., & Maaref, H. (2021). Electrical behavior of n-GaAs based Schottky diode for different contacts: Temperature dependence of c urrent-voltage. International Journal of Numerical Modelling: Electronic Networks, Devices and Fields, 34(6), e2916. doi: https://doi.org/10.1002/jnm.2916

Helal, H., Benamara, Z., Kacha, A. H., Amrani, M., Rabehi, A., Akkal, B., ... & Robert-Goumet, C. (2019). Comparative study of ionic bombardment and heat treatment on the electrical behavior of Au/GaN/n-GaAs Schottky diodes. Superlattices and Microstructures, 135, 106276. doi: https://doi.org/10.1016/j.spmi.2019.106276

Helal, H., Benamara, Z., Pérez, B. G., Kacha, A. H., Rabehi, A., Wederni, M. A., ... & Robert-Goumet, C. (2020). A new model of thermionic emission mechanism for non-ideal Schottky

contacts and a method of extracting electrical parameters. The European Physical Journal Plus, 135(11), 895. doi: https://doi.org/10.1140/epjp/s13360-020-00916-5

Kacha, A. H., Akkal, B., Benamara, Z., Robert-Goumet, C., Monier, G., & Gruzza, B. (2016). Study of the surface state density and potential in MIS diode Schottky using the surface photovoltage method. Molecular Crystals and Liquid Crystals, 627(1), 66-73. doi: https://doi.org/10.1080/15421406.2015.1137114

Law, M., Sirbuly, D. J., Johnson, J. C., Goldberger, J., Saykally, R. J., & Yang, P. (2004). Nanoribbon waveguides for subwavelength photonics integration. Science, 305(5688), 1269-1273. doi: https://doi.org/10.1126/science.1100999

Lin, Z., Gendry, M., & Letartre, X. (2014). Optical mode study of III–V-nanowire-based nanophotonic crystals for an integrated infrared band microlaser. Photonics Research, 2(6), 182-185. doi: https://doi.org/10.1364/PRJ.2.000182

Mayer, B., Rudolph, D., Schnell, J., Morkötter, S., Winnerl, J., Treu, J., ... & Finley, J. J. (2013). Lasing from individual GaAs-AlGaAs core-shell nanowires up to room temperature. Nature communications, 4(1), 2931. doi: https://doi.org/10.1038/ncomms3931

Núñez, C. G., Braña, A. F., López, N., Pau, J. L., & García, B. J. (2020). Single GaAs nanowire based photodetector fabricated by dielectrophoresis. Nanotechnology, 31(22), 225604. doi: 10.1088/1361-6528/ab76ee

Pauzauskie, P. J., & Yang, P. (2006). Nanowire photonics. Materials today, 9(10), 36-45. doi: https://doi.org/10.1016/S1369-7021(06)71652-2

Rhoderick, E. H., & Williams, R. H. (1988). Metal-semiconductor contacts (Vol. 252). Oxford: Clarendon press. doi: 10.1049/ip-i-1.1982.0001

Saxena, D., Mokkapati, S., Parkinson, P., Jiang, N., Gao, Q., Tan, H. H., & Jagadish, C. (2013). Optically pumped room-temperature GaAs nanowire lasers. Nature photonics, 7(12), 963-968. doi: https://doi.org/10.1038/nphoton.2013.303

Selberherr, S. (1984). Analysis and simulation of semiconductor devices. Springer Science & Business Media. doi: https://books.google.dz/books?id=EE4HlRZTYi4C

Selberherr, S. (1984). Process and device modeling for VISI. microelectronics reliability, 24(2), 225-257. doi: https://doi.org/10.1016/0026-2714(84)90450-5

Sze, S. M., Li, Y., & Ng, K. K. (2021). *Physics of semiconductor devices*. John wiley & sons. doi: http://hdl.handle.net/123456789/106

Wang, H. (2013). High gain single GaAs nanowire photodetector. Applied Physics Letters, 103(9), 093101. doi: https://doi.org/10.1063/1.4816246

Wu, Y., Yan, X., Zhang, X., & Ren, X. (2016). A monolayer graphene/GaAs nanowire array Schottky junction self-powered photodetector. Applied Physics Letters, 109(18), 183101. doi: https://doi.org/10.1063/1.4966899

Yan, R., Gargas, D., & Yang, P. (2009). Nanowire photonics. Nature photonics, 3(10), 569-576.

Yang, P., Yan, R., & Fardy, M. (2010). Semiconductor nanowire: what's next?. Nano letters, 10(5), 1529-1536. doi: https://pubs.acs.org/doi/abs/10.1021/nl100665r